Recovery of Cobalt and Nickel from Acidic Waste Streams: Effect of Chloride, Sulfate and Column Studies Using Phosphonic Acid Functionalised Silica

J. T. M. Amphlett, S. E. Pepper, W. Peng, M. D. Ogden*

Separations and Nuclear Chemical Engineering Research (SNUCER), Department of Chemical and Biological Engineering, The University of Sheffield, Sheffield, United Kingdom

**Corresponding author: m.d.ogden@sheffield.ac.uk*

Cobalt and nickel are common elements found in contaminated water from many industries, one of those being mining. Both of these elements are considered to be harmful, even at low concentration. This means that the ingress of these elements into the natural environment must be prevented and, if it has occurred, the contaminated water must undergo a remediation process. This research has focussed on the use of ethyl/butyl phosphonate silica for the recovery of low concentrations of Co^{2+} and Ni^{2+} from HCl solutions with increasing $[Cl^-]$ and $[SO_4^{2-}]$ in a batch system, as well as Co^{2+} and Ni^{2+} recovery from HCl in a column system. Single-element studies were performed to determine extractant behaviour under simple column loading conditions, followed by mixed Co/Ni systems to assess competition. Breakthrough curves have been fitted to various mathematical models to help understand fundamental behaviour and aid in potential process scale up.

INTRODUCTION

Cobalt and nickel are endemic to modern day society, with many uses including as additives in steel to give better corrosion and heat resistance (Bauer *et al*., 2010; Zinkle and Was, 2013), as major components of batteries (Naoko *et al*., 2015), in pigments and inks (Gotoh *et al*., 2007) and in medicine (Jacobs *et al*., 1998). Use in these industries can result in the release of Co and Ni into the environment through effluent discharge and leaching of industrial waste. Another major route for ingress of these elements into the environment is from their mining and mining-related processes, such as acid mine drainage (Suponic and Blanco, 2014). For example, soils samples around the Selebi–Phikwe Cu–Ni mine in Botswana have been shown to contain up to 266.6 mg kg^{-1} of Ni (Ekosse and Ngole, 2012), exceeding threshold and guideline values for soil (Tóth *et al*., 2016). This increased concentration of these metals in the environment has detrimental effects on animal and plant life due to their toxicities (Pepper *et al*., 2017).

To prevent the detrimental effects of Co and Ni on living organisms they must be removed and safely immobilised, either from the contaminated environment in a remediation process, or from effluent in a preventative process before environmental contamination can occur. Commonly employed methods for metal removal from aqueous solutions are precipitation/filtration, solvent extraction (SX) and ion exchange (IX) (Alexandratos, 2009; Ritcey and Ashbrook, 1984). Though there are advantages to each method, it is thought that IX is the most suitable method for the immobilisation of problematic species in effluent waste streams. Advantages of IX over SX include not producing large amounts of potentially toxic and flammable secondary waste, being better suited for extraction from low

concentration aqueous phases and the removal of problems associated with phase separation and third-phase formation (Amphlett *et al*., 2018; Veliscek-Carolan, 2016). The major advantage for the scenario discussed in this paper of IX over precipitation/filtration is that it can be done in a continuous flow through system, without the complication of needing to hold effluent waste in tanks while chemicals are added to facilitate precipitation.

There has been much recent work looking at the use of IX materials of different types for the recovery of cobalt and nickel from various aqueous matrices, with many having structures based around organic polymers or inorganic silica (Hanzel and Rajec, 2000; Pepper *et a*l., 2017; Sirola *et a*l., 2008; Sofińska-Chmiel and Kołodyńska, 2016; Xie *et al*., 2008). Though both structures have their merits, organic polymeric resins can show slow kinetics, may swell, be sensitive to chemical environments and lose mechanical stability (Pepper *et al*., 2017). As well as the potential to regenerate the silica extractants, there is the option of converting them directly into a stable glass waste form which can easily be disposed of.

Previously, ethyl/butyl phosphonate functionalised silica (EBP-Si) (Figure 1) has been investigated for its extraction capability towards Ni^{2+} and Co^{2+} (alongside aminophosphonic acid resin Puromet MTS9500) using batch techniques to assess maximum loading capacities and uptake kinetics (Pepper *et al*., 2017). EBP-Si showed maximum loading capacities of 4.43 g L_{Si}^{-1} and 2.39 g L_{Si}^{-1}, respectively, for Co^{2+} and Ni^{2+}. This is lower than values reported for Puromet MTS9500 (9.01 and 4.86 g L_{resin}^{-1}, respectively), which is due to S950 being macroporous and therefore having more sorption sites than EBP-Si, which is surface functionalised. However, EBP-Si was shown to have much faster kinetics than macroporous S950, with rate constants of 14.51 and 20.17 g mol^{-1} min^{-1} for Co^{2+} and Ni^{2+}, respectively, compared with 5.50 and 5.59 g mol^{-1} min^{-1} for S950 (predicted from a pseudo-second-order model fit).

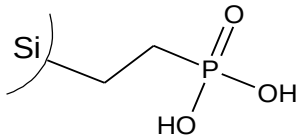

Figure 1: Functionality of EBP-Si.

This paper takes the previously reported work forwards and looks at the behaviour of EBP-Si towards Co^{2+} and Ni^{2+} extraction under increasing chloride and sulfate concentrations, as well as in a column loading system. Though the macroporous S9500 resin showed higher loading capacities (Pepper *et al*., 2017), the advantages of faster kinetics and ease of final disposal of the silica system warranted further investigation.

EXPERIMENTAL

Equipment and Reagents

All chemicals were purchased from Sigma-Aldrich and used as received. Solutions of Co^{2+} and Ni^{2+} were prepared using deionised water (> 18 MΩ).

Effect of Chloride and Sulfate

Wet EBP-Si (1.5 mL) was added contacted with solution containing Co^{2+} or Ni^{2+} (100 mg L^{-1}) at pH 2 (HCl) with varying concentrations of Cl^- or SO_4^{2-} (0.1–4.0 M, as NaCl or $(NH_4)_2SO_4$). Mixtures were agitated on an orbital shaker overnight followed by sampling of the resulting solution for analysis using atomic absorption spectroscopy (Perkin Elmer Atomic Absorption Spectrometer AAnalyst 400).

Column Loading Experiments

Wet EBP-Si (1.2 mL) was added to a column (12 mm internal diameter, 90 mm height) and solutions containing Co^{2+} or Ni^{2+} or Co^{2+} and Ni^{2+} (100 mg L^{-1} of each metal, pH 2 HCl) were pumped through

at a flow rate of 4 bed volumes per hour (BV h^{-1}). Effluent from the column was collected at set time intervals using a fraction collector and analysed for metal concentration using atomic absorption spectroscopy (Perkin Elmer Atomic Absorption Spectrometer AAnalyst 400).

RESULTS AND DISCUSSION

Effect of Chloride and Sulfate

Increasing [Cl−] and [SO_4^{2-}] were both observed to suppress Co^{2+} and Ni^{2+} uptake significantly (Figures 2 and 3). It can be seen that increasing [Cl^-] has a more pronounced effect on the recovery of both Ni^{2+} and Co^{2+}. This comes around for two reasons. Firstly, the competition between the extraction of Co^{2+}/Ni^{2+} by EBP-Si and the formation of aqueous chloride or sulfate species, and secondly, the buffering effect of SO_4^{2-} through its ability to sequester H^+ from solution and EBP-Si. It is also evident that Co^{2+} has a higher affinity for EBP-Si than Ni^{2+}.

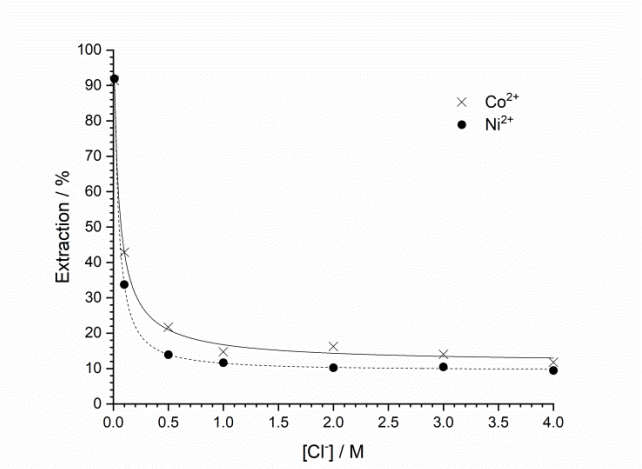

Figure 2: Extraction of Co^{2+} and Ni^{2+} from aqueous solution (pH 2 HCl) with increasing Cl^- (added as NaCl) concentration using EBP-Si. Lines present to guide the eye only.

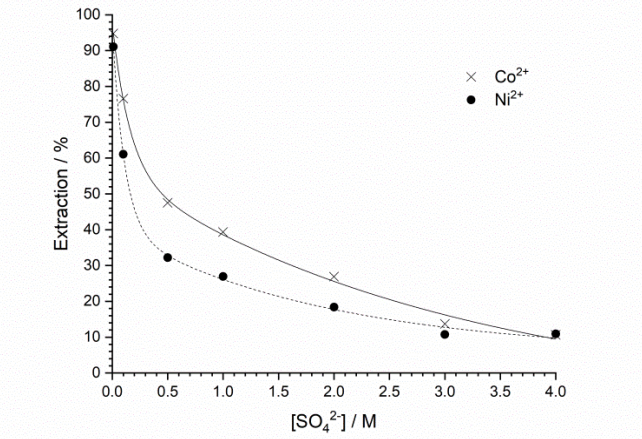

Figure 3: Extraction of Co^{2+} and Ni^{2+} from aqueous solution (pH 2 HCl) with increasing SO_4^{2-} concentration using EBP-Si. Lines present to guide the eye only.

Coordination of aqueous Ni^{2+} and Co^{2+} should be more favorable with SO_4^{2-} than with Cl^- (Equations 1–4) (Martell *et al*., 2004). However, if this coordination was the dominant process in solution then uptake suppression should occur more readily in sulfate media, which is the opposite of what is observed. This may seem counterintuitive, however, log *k* for the association of SO_4^{2-} with a proton is 0.93 (Martell *et al*., 2004), which means that the formation of HSO_4^- will happen in preference to metal

ion complexation by SO_4^{2-}. This ability to abstract H^+ from solution will also help to drive the extraction of Ni^{2+} and Co^{2+} by EBP-Si, as extraction of these metals happens due to ion exchange and acid dissociation at the silica surface (Pepper *et al*., 2017). The complexity of the sulfate system in comparison with the chloride system can be seen when slope analysis is attempted, a standard tool for understanding such processes. Plots of pH against log k_D in chloride media give straight lines with gradients of 2.6 and 2.3 for Co^{2+} and Ni^{2+}, respectively, whereas in sulfate media slope analysis plots do not produce straight lines.

$$Co^{2+} + Cl^- \rightarrow [CoCl]^+ \qquad \log k = -0.28 \qquad [1]$$

$$Co^{2+} + SO_4^{2-} \rightarrow CoSO_4 \qquad \log k = 0.23 \qquad [2]$$

$$Ni^{2+} + Cl^- \rightarrow [NiCl]^+ \qquad \log k = -0.64 \qquad [3]$$

$$Ni^{2+} + SO_4^{2-} \rightarrow NiSO_4 \qquad \log k = 0.26 \qquad [4]$$

The salts used to increase $[SO_4^{2-}]$ and $[Cl^-]$ ($(NH_4)_2SO_4$ and NaCl) will also have an effect on the extraction of Co^{2+} and Ni^{2+}. Na^+ will compete more effectively than NH_4^+ for sites on EBP-Si with Co^{2+} and Ni^{2+}. It is also bound more strongly than H^+, as evidenced by a decrease in Co^{2+} and Ni^{2+} uptake of 10–12% when using the Na form of EBP-Si as opposed to the H^+ form. This is likely what accounts for the more drastic initial suppression of metal recovery in the chloride system.

Column Loading Behaviour

Breakthrough curves were produced from collected data by plotting the ratio of the effluent $[Co^{2+}]$ or $[Ni^{2+}]$ to their influent concentrations (C/C_i) against effluent volume in bed volumes (BV) (Figure 3). The breakthrough curves were used to calculate: breakthrough volume (B_v, BV), which is the volume of influent passed through the column before target solute is either detectable or above a desired level in the effluent stream; resin breakthrough capacity (B_{cap}, mg), which is the amount of target solute sorbed on the resin before breakthrough occurs; time to 50% breakthrough (t_{50}, min), which the time to where C/C_i = 0.5; volume to 50% breakthrough (BV_{50}, BV); which is the influent volume passed through the column to achieve C/C_i = 0.5; and resin saturation capacity (q_m, mg mL_{wsr}^{-1}), which is the loading capacity of the resin towards the target solute (see Table I).

Table I: Calculated values of B_v, B_{cap}, t_{50}, BV_{50} *and* q_m *for* Ni^{2+} *and* Co^{2+} *(100 mg* L^{-1}*) loading onto EBP-Si from pH 2 HCl at a flow rate of 4 BV* h^{-1}.

	Co^{2+}	Ni^{2+}
B_v (BV)	32	24
B_{cap} (mg g^{-1})	6.43	4.82
t_{50} (h)	10.5	7.5
BV_{50} (BV)	42	30
q_m (mg g^{-1})	14.11	10.07

The breakthrough curves (Figure 3) and associated metal loading parameters (Table II) show that Co^{2+} is extracted to the resin more strongly than Ni^{2+}, agreeing with data collected in the static experiments (Figures 1 and 2). It is currently not explicitly known why there is such a difference in affinity between the two metals towards EBP-Si. This difference may be due to differences in the stability of the two metal–ligand complexes; however, log stability constants for ethylphosphonic acid binding with Co^{2+} and Ni^{2+} are reported at similar values of 2.27 and 2.30, respectively (Martell *et al*., 2004; Straiak *et a*l., 1992). It must be noted, however, that values were measured in the aqueous phase and are likely not the same as in the system studied in this work due to the act of tethering the functionality to the silica surface.

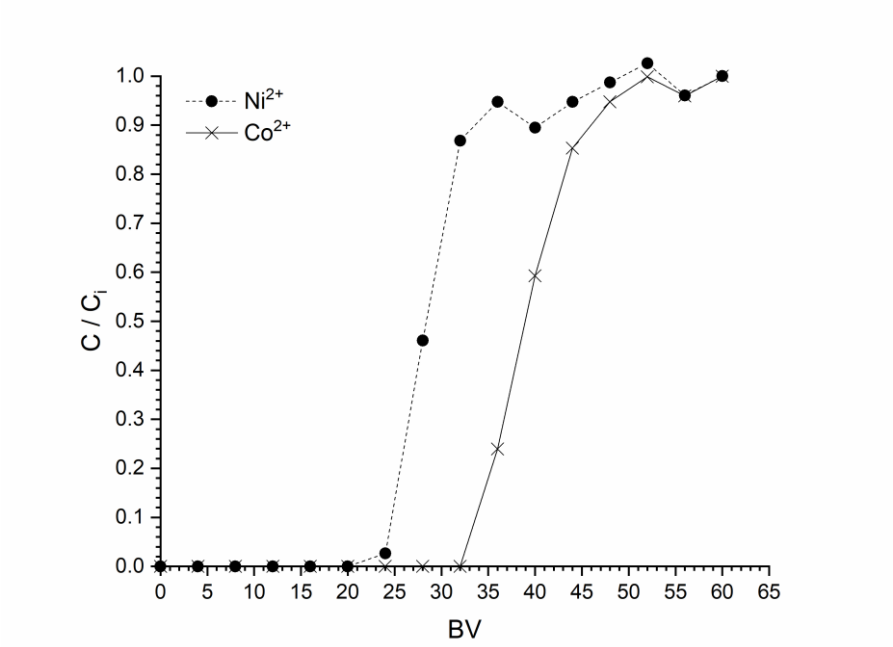

Figure 3: Column loading of Ni^{2+} and Co^{2+} on to EBP-Si at pH 2 (HCl) and a flow rate of 4 BV h^{-1}.

There are multiple models available in the literature that can be used to predict the breakthrough behaviour of IX resins towards aqueous metal species. For the purpose of this work, the Yoon–Nelson (Yoon & Nelson, 1984), Thomas (Thomas, 1944) and modified dose-response (Yan *et al*., 2001) have been used. It must be noted, however, that these models were not necessarily derived using the theoretical basis of IX chemistry, and therefore the extracted parameters may not be representative of the real experiment. These models primarily allow for comparison with current literature data. All model fitting was carried out via linear regression analysis using *Origin Pro 2015*, with errors being calculated at a 95% confidence interval from standard errors given by the line of best fit.

Yoon–Nelson

The Yoon–Nelson model was derived to model gaseous adsorption onto solid sorbent respirator cartridges (Yoon & Nelson, 1984). It is based on the on the assumption that the rate of decrease in the probability of adsorption is proportional to the probability of the adsorbate adsorption and the adsorbate breakthrough on the adsorbent (Calero *et al*., 2009; Tavakoli *et al*., 2013). The linear and non-linear equations for this model are shown in [5] and [6], respectively, where K_{YN} is the Yoon–Nelson constant (min^{-1}).

$$ln\left(\frac{C_i}{C}\right) = K_{YN}t_{50} - K_{YN}t \quad [5]$$

$$\frac{C}{C_i} = \frac{1}{1+e^{K_{YN}(t_{50}-t)}} \quad [6]$$

Thomas

The Thomas model was derived to explain column loading of aqueous species onto a zeolite (Thomas, 1944). It is based on the assumption that uptake is not controlled by chemical equilibria, but by mass transfer at the interface between the resin and the aqueous matrix (Calero *et al*., 2009; Tavakoli *et al*., 2013). The linear and non-linear equations from this model are shown in [7] and [8], respectively, where K_{TH} is the Thomas constant (L min^{-1} mg^{-1}), m is the mass of the resin in the column (g), Q is the flowrate (ml min^{-1}) and V_{ef} is the effluent volume (mL).

$$ln\left(\frac{C_i}{C} - 1\right) = \left(\frac{K_{TH}}{Q}\right)(q_m m) - \left(\frac{K_{TH}}{Q}\right)(C_i V_{ef}) \quad [7]$$

$$\frac{C}{C_i} = \frac{1}{1+e^{\left(\frac{K_{TH}}{Q}\right)\left(q_m m - C_i V_{eff}\right)}} \quad [8]$$

Modified dose-response

The modified dose-response model (Yan *et al*., 2001) is based on the dose-response model which has historically been used in the fields of medicine and pharmacology. The linear and non-linear forms of the equation are shown in [9] and [10], respectively, where *a* and *b* are modified dose-response model constants. By equating [11] to 50% removal (C/C_i = 0.5) and applying the Thomas model, it is possible to produce an expression to calculate q_m [10].

$$ln\left(\frac{C_i}{C} - 1\right) = a\, ln(b) - a\, ln\left(V_{ef}\right) \quad [9]$$

$$\frac{C}{C_i} = 1 - \frac{1}{1+\left(\frac{V_{ef}}{b}\right)^a} \quad [10]$$

$$q_m = \frac{bC_i}{m} \quad [11]$$

Fitting parameters for each of the models are presented in Table II. All the models are able to adequately reproduce breakthrough curves for Co^{2+} and Ni^{2+} on EBP-Si. The modified dose-response model fits best, however R^2 values are very similar for all the models. Maximum loading capacities predicted from the modified dose-response model are lower than those calculated from experimental data, with values of 8.43 and 6.02 mg g^{-1} (calculated), compared with 6.23 and 5.70 mg g^{-1} (fit) for Co^{2+} and Ni^{2+}, respectively. The same trend is seen with t_{50}, predicted by the Yoon–Nelson model. Predictions are lower than the calculated values.

Table II: Fitting parameters for the Yoon-Nelson, Thomas, and modified dose-response models.

	Yoon–Nelson			Thomas			Modified dose-response			
	R^2	K_{YN}	t_{50} (h)	R^2	K_{TH} (L h^{-1} mg^{-1})	q_m (mg g^{-1})	R^2	*a*	*b*	q_m (mg g^{-1})
Co^{2+}	0.998	1.578 ± 0.089	9.503 ± 0.045	0.998	0.066 ± 0.004	7.865 ± 0.033	0.999	15.251 ± 0.695	46.867 ± 0.160	8.01
Ni^{2+}	0.994	2.301 ± 0.312	6.746 ± 0.062	0.994	0.096 ± 0.013	5.710 ± 0.049	0.995	15.875 ± 1.980	34.066 ± 0.276	5.70

Competition Studies

Experiments were conducted with Co^{2+} and Ni^{2+} being extracted by EBP-Si at the same time. Breakthrough curves for these data are presented in Figure 4, with calculated parameters shown in Table III. It can be seen that breakthrough occurs sooner for this system than it does with the single metal systems. The calculated parameters in Table III are roughly half of those seen in Table I. However, Co^{2+} and Ni^{2+} appear to behave in a similar fashion, which is not what was seen with the individual systems where Co^{2+} had a higher loading capacity then Ni^{2+} (14.11 mg g^{-1} *vs*. 10.02 mg g^{-1}, respectively). The collected data were fit with the previously discussed breakthrough models, with fit parameters shown in Table IV. As with the individual metal systems, all the models adequately fit the data with R^2 values of 0.996 or above.

Table III: Calculated values of B_v, B_{cap}, t_{50}, BV_{50} *and* q_m *for* Ni^{2+} *and* Co^{2+} *(100 mg* L^{-1}*) loading onto EBP-Si from pH 2 HCl at a flow rate of 4 BV* h^{-1}.

	Co^{2+}	Ni^{2+}
B_v (BV)	17	17
B_{cap} (mg g^{-1})	3.41	3.41
t_{50} (h)	5.68	5.68
BV_{50} (BV)	22.72	22.72
q_m (mg g^{-1})	6.25	6.25

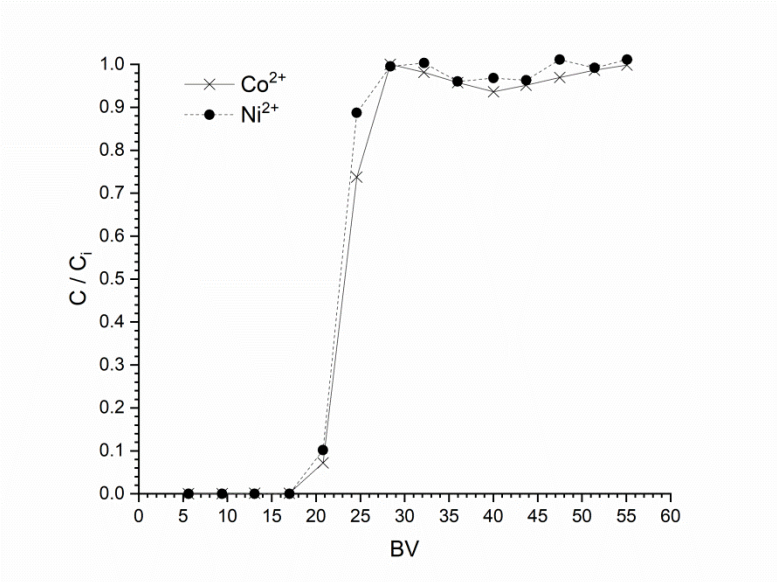

Figure 4: Column loading of Ni^{2+} and Co^{2+} on to EBP-Si at pH 2 (HCl) and a flow rate of 4 BV h^{-1}.

Table IV: Fitting parameters for the Yoon–Nelson, Thomas, and modified dose-response models.

	Yoon–Nelson			Thomas			Modified dose-response			
	R^2	K_{YN}	t_{50} (h)	R^2	K_{TH} (L h^{-1} mg^{-1})	q_m (mg g^{-1})	R^2	a	b	q_m (mg g^{-1})
Co^{2+}	0.996	3.806 ± 0.485	5.525 ± 0.049	0.996	0.186 ± 0.012	4.720 ± 0.034	0.996	21.691 ± 2.757	28.128 ± 0.214	4.71
Ni^{2+}	0.998	4.464 ± 0.300	5.352 ± 0.033	0.998	0.096 ± 0.013	4.568 ± 0.025	0.998	25.271 ± 1.676	24.205 ± 0.150	4.05

CONCLUSIONS

Phosphonate-functionalised silica EBP-Si has been shown to be able to extract Co^{2+} and Ni^{2+} from HCl media, with Co^{2+} showing a greater affinity for the resin then Ni^{2+}. The presence of Cl^- and SO_4^{2-} causes suppression of uptake, along with the presence of Na^+. However, the effect of SO_4^{2-} in the absence of Na^+, through the use of NH_4Cl does need to be investigated. This trend is also shown when extracting under column loading conditions, where Co^{2+} extraction gives higher breakthrough volumes and loading capacities. Sharp breakthrough curves indicate fast kinetics, as seen in previous work (Pepper *et al*., 2017), and warrants further experimentation at higher flowrates.

All the breakthrough models used were able to adequately fit breakthrough data, from single- and mixed-metal systems. This shows that these models may be effective in predicting breakthrough behaviour when moving from simple to more complex aqueous matrices; however, the fact that they all fit may be a comment on their lack of specificity for such extraction systems.

More work is needed to investigate the applicability of Si based extractants towards Co^{2+} and Ni^{2+} recovery. This initial work suggests that they show promise, though the low loading capacities seen would currently be a barrier to their implementation. EBP-Si is not overly expensive in comparison to commercially available plastic IX resins, being GBP 101 for 10 g. It is also likely that this will have a longer lifetime that traditional resins, as its inability to swell removes associated problems (e.g., osmotic shock) and its harder surface should be more resistant to abrasion and physical damage. To take this work further, a macroporous silica backbone should be used, to increase surface area and likely increase loading capacity closer to what could be seen for a macroporous polystyrenic resin, as well as conducting elution testing.

ACKNOWLEDGEMENTS

Special thanks to Claire Corkhill and Clare Thorpe for their help with ICP-OES analysis and Mark Jones for his assistance with AAS. This work was supported by the Engineering and Physical Sciences Research Council through the UK Korea Civil Nuclear Energy program grant EP/M026558/1 Silicate Nanoparticles for Extraction of Radionuclides (SINNER). We would also like to thank the referees for their insightful comments towards this paper.

REFERENCES

Alexandratos, S.D. (2009). Ion-exchange resins: A retrospective from industrial and engineering chemistry research. *Industrial & Engineering Chemistry Research*, 48, 388–398.

Amphlett, J.T.M., Ogden, M.D., Foster, R.I., Syna, N., Soldenhoff, K.H., Sharrad, C.A. (2018). Polyamine functionalised ion exchange resins: synthesis, characterisation and uranyl uptake. *Chemical Engineering Journal*, 334, 1361–1370.

Bauer, A., Neumeier, S., Pyczak, F., Goken, M. (2010). Microstructure and creep strength of different gamma/gamma'-strengthened Co-base superalloy variants. *Scripta Materialia*, 63, 1197–1200.

Calero, M., Hernáinz, F., Blázquez, G., Tenorio, G., artín-Lara, M.A. (2009). Study of Cr (III) biosorption in a fixed-bed column. *Journal of Hazardous Materials*, 171(1–3), 886–893.

Ekosse, G.I.E., Ngole, V.M. (2012). Copper, nickel and zinc contamination in soils within the precincts of mining and landfilling environments. *International Journal of Environmental Science and Technology*, 9, 485–494.

Gotoh, A., Uchida, H., Ishizaki, M., Satoh, T., Kaga, S., Okamoto, S., Kurihara, M. (2007). Simple synthesis of three primary colour nanoparticle inks of Prussian blue and its analogues. *Nanotechnology*, 18 (34), 345609.

Hanzel, R., Rajec, P. (2000). Sorption of cobalt on modified silica gel materials. *Journal of Radioanalytical and Nuclear Chemistry*, 246(3), 607–615.

Jacobs, J.J., Gilbert, J.L., Urbant, R.M. (1998). Current concepts review corrosion of metal oOrthopaedic implants. *Journal of Bone and Joint Surgery*, 80(2), 268–282.

Martell, A.E., Smith, R.S., Motekaitis, R.J. (2004). NIST critically selected stability constants of metal complexes. *NIST Standard Reference Database*, 8.

Naoki, N., Feixiang, W., Jung Tae, L., Gleb, Y. (2015). Li-ion battery materials: present and future. *Materials Today*, 18(5), 252–264.

Pepper, S.E., Whittle, K.R., Harwood, L.M., Cowell, J., Lee, S., Ogden, M.D., Cobalt, M.D.O. (2017). Cobalt and nickel uptake by silica-based extractants. *Separation Science and Technology*, 53(4), 1–11.

Ritcey, G.M., Ashbrook, A. W. (1984). *Solvent Extraction: Principles and Applications to Process Metallurgy*. Elsevier, Amsterdam.

Sirola, K., Laatikainen, M., Lahtinen, M., Paatero, E. (2008). Removal of copper and nickel from concentrated $ZnSO_4$ solutions with silica-supported chelating adsorbents. *Separation and Purification Technology*, 64, 88–100.

Sofińska-Chmiel, W., Kołodyńska, D. (2016). Purolite S940 and Purolite S950 in heavy metal ions removal from acidic streams. *Separation Science and Technology*, 51 (15–16), 2528–2538.

Straiak, M., Massoud, S.S., Sigel, H. (1992). Metal ion coordinating properties of various phosphonate derivatives, including 9-[2-(phosphonylmethoxy)ethyl]adenine (PMEA)-an adenosine monophosphate (AMP) analogue with antiviral properties. *Helvetica Chimica Acta*, 75, 2634–2656.

Suponic, T., Blanco, M. (2014). Removal of heavy metals from groundwater affected by acid mine drainage. *Physicochemical Problems of Mineral Processing*, 50(1), 359–372.

Tavakoli, H., Sepehrian, H., Semnani, F., Samadfam, M. (2013). Recovery of uranium from UCF liquid waste by anion exchange resin CG-400: Breakthrough curves, elution behavior and modeling studies. *Annals of Nuclear Energy*, 54, 149–153.

Thomas, H.C. (1944). Heterogeneous ion exchange in a flowing system. *Journal of the American Chemical Society*, 66 (10), 1664–1666.

Tóth, G., Hermann, T., Silva, M.R.Da., Montanarella, L. (2016). Heavy metals in agricultural soils of the European Union with implica- tions for food safety. *Environment International*, 88, 299–309.

Veliscek-Carolan, J. (2016). Separation of actinides from spent nuclear fuel: A review. *Journal of Hazardous Materials*, 318, 266–281.

Xie, F., Lin, X., Wu, X., Xie, Z. (2008). Solid phase extraction of lead (II), copper (II), cadmium (II) and nickel (II) using gallic acid-modified silica gel prior to determination by flame atomic absorption spectrometry. *Talanta*, 74, 836–843.

Yan, G., Viraraghavan, T., Chen, M. (2001). A new model for heavy metal removal in a biosorption column. *Adsorption Science & Technology*, 19 (1), 25–43.

Yoon, Y.H., Nelson, J.H. (1984). Application of gas-adsorption kinetics. I. A theoretical model for respirator cartridge service life. *American Industrial Hygiene Association Journal*, 45 (8), 509–516.

Zinkle, S.J., Was, G.S. (2013). Materials challenges in nuclear energy. *Acta Materialia*, 61 (3), 735– 758.